



Contents lists available at ScienceDirect

Journal of King Saud University – Science

journal homepage: www.sciencedirect.com

Original article

Biological activities of chitosan-salicylaldehyde schiff base assisted silver nanoparticles

Salman S. Alharthi^{a,1}, Thandapani Gomathi^{b,1,*}, J. John Joseph^c, J. Rakshavi^b, J. Annie Kamala Florence^d, Prasad N. Sudha^b, Govindasamy Rajakumar^e, Muthu Thiruvengadam^{f,*}^a Department of Chemistry, College of Science, Taif University, P.O. Box 110999, Taif 21944, Saudi Arabia^b PG and Research Department of Chemistry, D.K.M. College for Women, Vellore, Tamil Nadu, India^c VIT TBI, VIT University, Vellore, Tamil Nadu, India^d Department of Chemistry, Voorhees College, Vellore, Tamil Nadu, India^e Collaborative Innovation Center for Advanced Organic Chemical Materials Co-Constructed by the Province and Ministry, Ministry of Education Key Laboratory for the Synthesis and Application of Organic Functional Molecules, College of Chemistry and Chemical Engineering, Hubei University, Wuhan 430062, China^f Department of Crop Science, College of Sanghuh Life Science, Konkuk University, Seoul 05029, Republic of Korea

ARTICLE INFO

Article history:

Received 31 March 2022

Revised 24 May 2022

Accepted 9 June 2022

Available online 15 June 2022

Keywords:

Silver nanoparticles

Chitosan

Schiff base

Salicylaldehyde

Biological assay

Biosafety assay

ABSTRACT

Objectives: The nanobiotechnology era has sparked interest in the green synthesis of stable silver nanoparticles (Ag-NPs) without hazardous chemicals. As a result, the current study used chitosan-salicylaldehyde Schiff base (CSB) as a non-toxic, reducing and stabilizing agent to prepare stable silver nanoparticles.

Methods: The characterization of Ag-NPs impregnated chitosan-salicylaldehyde Schiff base was fulfilled using UV-Vis, FTIR, XRD and TEM studies.

Results: The absorption band present around 425 nm in UV-Vis spectra indicated the formation of Ag-NPs. The appearance of a new band for the C=N bond, deduction in the intensity of the C=O group of salicylaldehyde and N-H group of chitosan confirmed the formation of Schiff base and Ag-NPs in FTIR analysis. XRD pattern revealed the orientation and crystalline nature of Ag-NPs with 2θ at 38° , 46° and 54° related to Ag-NPs (JCPDS No. 04-0783), whereas the peak at $2\theta = 27^\circ$ associated with CSB. The total porosity of 53.24% was determined using the liquid displacement method. The CSB-Ag-NPs have good scavenging activity (46.25% and 49.35% activity in DPPH assay and H_2O_2 assay), great antibacterial (zone of inhibition 17 mm and 19 mm for *E-Coli* and *Pseudomonas* sp.), antifungal (18 mm for *P. notatum*), and anti-larvicidal activity, according to biological assessments.

Conclusions: The synthesised Ag-NPs were non-toxic to marine ecosystems in a safety bioassay test.

© 2022 The Author(s). Published by Elsevier B.V. on behalf of King Saud University. This is an open access article under the CC BY license (<http://creativecommons.org/licenses/by/4.0/>).

1. Introduction

Chitosan is deacetylated product of chitin, having biodegradable and non-toxic properties (Hataf et al., 2018). The behavioural study of chitosan towards lysozyme, an enzyme prevalent in

human body fluids that digests chitosan, resulted in enhanced uses of chitosan in biomedical, pharmacological, agricultural, and environmental domains (Dutta et al., 2004; Badawy et al., 2019). Chitosan is a remarkable material in dialysis and has fungistatic, bacteriostatic, anticancer and anticholesteremic properties (Dutta et al., 2004). The free amino group at the C2 position of chitosan makes it more available for reaction to form derivatives with enhanced physicochemical properties. Especially, chitosan Schiff bases are considered one of the best options to increase the biological properties of unmodified chitosan.

An increase in antibacterial activity was observed with such derivatives due to changes in the molecular structure of chitosan, enhancement of hydrophilicity and increasing positively charged ions (Wang et al., 2020). Many studies revealed that the addition of chitosan improves plant growth and development without illnesses. It can boost the immune system in plant cells. Similarly,

* Corresponding authors.

E-mail addresses: chemist.goms@gmail.com (T. Gomathi), muthu@konkuk.ac.kr (M. Thiruvengadam).

¹ Salman S. Alharthi and Thandapani Gomathi are contributed equally to this work. Peer review under responsibility of King Saud University.



Production and hosting by Elsevier

<https://doi.org/10.1016/j.jksus.2022.102177>

1018-3647/© 2022 The Author(s). Published by Elsevier B.V. on behalf of King Saud University. This is an open access article under the CC BY license (<http://creativecommons.org/licenses/by/4.0/>).

chitosan and its derivatives participate in bacterial and fungal suppression for a safe human environment (Rezazadeh et al., 2020). Numerous chitosan Schiff bases have been developed, such as carboxymethyl chitosan Schiff bases, chitosan-crotonaldehyde, and chitosan-4-chlorobenzaldehyde Schiff bases examined for antibacterial and biological properties (Baran et al., 2015). Jin et al. (2009) synthesized a chitosan-citral Schiff base with enhanced antimicrobial activity than chitosan. Wang et al. (2009) synthesized Nano-chitosan (NCS), nano-chitosan salicylaldehyde Schiff-base (NCS-Sal), and nano-chitosan salicylaldehyde Schiff-base Cu complexes (NCS-Sal-Cu) which inhibited the growth of SMMC-7721 liver cancer cell lines. Guo et al. (2005) investigated the antioxidant property of carboxymethyl chitosan Schiff base. Similarly, Tong et al. (2005) synthesized CSB Co (II) and Pd (II) complexes and evaluated their high catalytic efficiencies.

Medically silver has proven antiseptic and antimicrobial activity against Gram + ve and Gram –ve bacteria. Also, silver nitrate solution has been used to prevent neonatal conjunctivitis (Le Ouay and Stellacci, 2015). Currently, silver nanoparticles are a promising and advanced option for developing efficient and remarkable antimicrobial systems to enhance therapeutic activities (Silver et al., 2006) that enhance cell surface permeation and adsorption at microbial surfaces (Le Ouay and Stellacci, 2015). Moreover, the broad-spectrum activity of silver nanoparticles makes them more available for application in a varied range of consumer products (He et al., 2016). Many polymers are used in the synthesis of silver nanoparticles. More specifically, chitosan has numerous roles in the synthesis, stability and use of nanoparticles (Susilowati and Maryani, 2019).

Ahmad et al. used chitosan and gelatin as the solid support for synthesizing silver nanoparticles (Bin Ahmad et al., 2011). The functional groups of chitosan act as chelating and reducing agents in silver nanoparticle production and prevent aggregation (Oves et al., 2021). So, in order to improve the biomedical properties and to demonstrate the biosafety of the silver nanoparticles, the use of non-toxic and biocompatible chitosan Schiff bases as a capping agent is an excellent option. The use of a polymer as a nanoparticle stabilizer is essential in preventing nanoparticle aggregation and improving biocompatibility qualities. Thus, the present research work addresses the synthesis of silver nanoparticles impregnated Chitosan-Salicylaldehyde Schiff base (CSB-Ag-NPs) and evaluated for its improved antibacterial spectrum, larvicidal activity, and biosafety assay.

2. Materials and methods

2.1. Materials

Chitosan was obtained from India Sea Foods, Cochin, Kerala, which is 92% deacetylated. Salicylaldehyde was procured from Sisco Research Laboratories Private Limited, Mumbai. Silver nitrate (Mol. wt 169.87) assay min, 99.8% ethanol was acquired. All the chemicals used were of the analytical grade and were obtained from Rechem Laboratory chemicals private Limited, Ambattur, Chennai. The egg and the egg raft of *Culex Quinquefasciatus* (*Cx. Quinquefasciatus*) were procured from the Zonal Entomological unit, Velapadi, Vellore, Tamil Nādu, India.

2.2. Preparation of chitosan Schiff base (CSB)

1 g of chitosan in 100 mL of 2% acetic acid solution was stirred under a magnetic stirrer for 30 min to get a homogeneous solution. 1 mL of salicylaldehyde dissolved in 15 mL of ethanol solution was added to this solution. It was further stirred on the magnetic stirrer for another 30 min. A yellow gel of Chitosan-Salicylaldehyde Schiff

base formed (Supriya Prasad et al., 2017). Then, the chitosan Schiff base gel was poured into a petri dish and allowed to dry for 48 h.

2.3. Preparation of CSB-Ag-NPs

0.2 g of prepared CSB was dissolved in 10 mL of double deionized water. To this solution, silver nitrate solution (0.05 g in 10 mL of ethanol) was added at 60 °C under magnetic stirring and the process was continued for 12 h. The color change was observed during the formation of silver nanoparticles, and it was confirmed by the formation of a brown color precipitate (Supriya Prasad et al., 2017). Then the precipitate was filtered and dried in a vacuum.

2.4. Characterization

The formation of CSB-Ag-NPs was confirmed by recording 200–800 nm spectra using a UV visible spectrophotometer (HITACHI-U2800). FTIR spectra of CSB and CSB-Ag-NPs have been recorded on Thermo Nicolet AVATAR 330 Spectrophotometer at room temperature within 4000 to 400 cm⁻¹ wavenumber using the KBr pellet method. The physical nature (amorphous or crystalline) of synthesized CSB-Ag-NPs was determined by using an x-ray powder diffractometer (XRD-SHIMADZU XD-D1) using Ni-filter, Cu-K_α radiation source and scattering range 2θ, varying from 10° to 90°. TEM image of the prepared CSB-Ag-NPs was recorded using a HITACHI-H-7650 transmission electron microscope.

2.5. Porosity measurements

The liquid displacement method was utilized to determine the total porosity of the prepared material. The volume of ethanol and sample was weighed initially before immersion. Then the weighted sample was immersed in dehydrated alcohol for 24 h and weighed again to measure the porosity using the following formula:

$$\% \text{ Porosity} = (V_2 - V_1 - V_3) / (V_2 - V_3) \times 100$$

Where V₁ = initial weight of the sample; V₂ = the sum of the weights of ethanol and the submerged sample and V₃ = the weight of ethanol after removal of the sample.

2.6. Antioxidant assay

2.6.1. DPPH scavenging activity

The stock solution was prepared by dissolving 10 mg of the sample (CS and CSB-Ag-NPs) in 10 mL of water and was made up to 50 mL in a standard flask. From the 50 mL stock solution, 1 to 6 mL was taken and made up to 10 mL in the test tubes using distilled water to get concentrations of 20, 40, 60, 80, 100 and 120 µg/mL. From these solutions, a 3 mL sample was pipette out into a test tube and 1 mL of 2, 2-diphenyl-1-picrylhydrazyl (DPPH) of normality 0.001 N was added. Then, it was kept in the darkroom for about 30 min and the absorbance was measured using a photo colorimeter (420 nm) with DPPH as the control. The scavenging percentage was calculated using the formula given below:

$$\% \text{ Scavenging} = \frac{A_{\text{control}} - A_{\text{sample}}}{A_{\text{control}}} * 100$$

2.6.2. Hydrogen peroxide scavenging activity

The stock solution was prepared by dissolving 10 mg of the sample (CS and CSB-Ag-NPs) in 10 mL of distilled water and was made up to 50 mL in a standard flask. From the 50 mL stock solution, 1 to 6 mL was taken and made up to 10 mL in the test tubes using distilled water to get concentrations of 20, 40, 60, 80, 100

and 120 µg/mL. A 3 mL sample was pipette out into a test tube from these solutions, and 1 mL H₂O₂ (40 g) produced in phosphate buffer (50 m pH 7.4) was added. In a photo colorimeter, the quantity of hydrogen peroxide was detected by absorption at 420 nm and the scavenging percentage was calculated using the formula given below:

$$\%Scavenging = \frac{A_{control} - A_{sample}}{A_{control}} * 100$$

2.7. Antimicrobial activity

By disc diffusion method utilizing Muller Hinton Agar (MHA) and Sabouraud Dextrose Agar (SDA) media, the antibacterial activity of the CSB-Ag-NPs was investigated against bacteria (*Escherichia coli*, *Pseudomonas aeruginosa*) and fungus species *Penicillium notatum*. MHA was incubated and sterilized in this technique by distributing it in a petri dish. After the MHA medium had solidified, a small portion of the sample was placed on various cultured agar plates. The plates were left at room temperature for 1 h to allow for diffusion of the compounds before being incubated at 37 °C for 24 h. The antibacterial activity was assessed by measuring the diameter of the inhibitory zone (mm). The antifungal activity of the CSB-Ag-NPs was investigated using a similar approach.

2.8. Larvicidal activity

Culex Quinquefasciatus (*Cx. Quinquefasciatus*) larvae were used in the larvicidal experiment. *Cx. Quinquefasciatus* eggs and egg rafts were placed in a 500 mL dechlorinated water container for 30–40 min, giving the larvae enough time to develop (Abdul Rahuman et al., 2008). The early fourth stage larvae were then used in a subsequent experiment. The technique was carried out in accordance with WHO recommendations, with certain modifications based on Santhosh kumar et al. technique (Santhoshkumar et al., 2011). A total of 20 larvae were immersed in 200 mL DD water containing 0.05 g, 0.03 g, and 0.2 g concentrations of CSB-Ag-NPs. After 24 h, the percentage of mortality was measured by counting the number of dead larvae in each batch.

2.9. Safety of CSB-Ag-NPs

The Brine Shrimp (*Artemia salina*) toxicity test was used to determine the biosafety of the CSB-Ag-NPs. To hatch the Brine Shrimp eggs under constant aeration for 48 h, artificial seawater (33 g/L sea salt adjusted to a pH of 8.5 using 1 M Na₂CO₃ solutions) was created in a sterile bottle. The hatching chamber's active nauplii were then collected and utilized. 10 shrimp were drawn via a glass capillary and deposited in a 6-well plate containing 5 mL Brine solution, as directed by the protocol (Hamidi et al., 2014). The sample was then put to wells at ambient temperature (37 °C) and flashed with visible light for 1, 2, 3, 4, and 24 h in the 100 L concentration using dimethyl sulfoxide (DMSO) (10, 100, 1000 g/mL). The dead larvae were counted. The percentage of mortality was determined using the following formula.

$$\%Mortality = \frac{NumberofdeadArtemiaNauplii}{TotalnumberofliveArtemiaNauplii} * 100$$

2.10. Statistical analysis

All the data was evaluated, and the average of three distinct numbers of individual observations was calculated. After 24 h of exposure, mortality was reordered as a mean percentage of *Artemia*

death. The mean and standard deviation are used to express the results.

3. Results and discussion

For every application of the prepared materials, their physico-chemical properties are essential for their efficacy. Therefore, knowing the properties of the synthesized material and characterization of CSB and CSB-Ag-NPs are significant to assessing the functional features of the material.

3.1. UV-Visible spectroscopy

The most reliable tool for examining the formation and stability of synthesized CSB-Ag-NPs is UV-Vis spectroscopy (Hamidi et al., 2014). The spectral properties of Ag-NPs are influenced by chemical environment, particle size and dielectric medium (Abdul Rahuman et al., 2008; Santhoshkumar et al., 2011). Because of the reducing agent CSB, the color of AgNO₃ was changed from colorless to dark brown, resulting in the synthesis of CSB-Ag-NPs. The maximum absorption spectrum was observed at 425 nm (Fig. 1), which was the characteristic absorption peak of Ag nanoparticles. Similar absorption peaks were reported in the range of 410–420 nm by other researchers (Wei et al., 2009). The shift in the UV absorbance was due to the chemical interaction of amine and aldehyde in CSB. According to the UV data, the silver nanoparticles were generated, and CSB worked as a capping and reducing agent. Using CSB as a capping and reducing agent, a UV-Vis analysis confirmed the formation of Ag-NPs.

3.2. FTIR analysis

FTIR analysis was performed to find out the presence and participation of functional groups of CSB in silver nanoparticle synthesis as a capping agent leading to efficient stabilization of the silver nanoparticles (Lin et al., 2014). Table 1, Fig. 2a and b represent the FTIR spectrum of CSB and CSB-Ag-NPs. The band corresponding to the wave numbers 3282 and 3265 cm⁻¹ represents N–H and O–H stretching vibrations. This band was observed as broadband due to the H bond interaction. The bands at around 2920–2870 cm⁻¹ correspond to C–H stretching modes of vibrations. The band at 1635 cm⁻¹ indicates the C=O stretching vibration of CSB, whereas it was observed at 1734 cm⁻¹ for CSB-Ag-NPs. The imine band observed at 1546 cm⁻¹ and 1589 cm⁻¹ for CSB and CSB-Ag-NPs, respectively, confirmed the formation of Schiff bases. The band's appearance at 1546 and 1589 cm⁻¹ can be attributed to the crosslinking reaction of chitosan and aldehyde. The characteristic band for the –NH₂ group almost disappeared, representing its participation in the reaction with the aromatic aldehyde to form Schiff bases.

In CSB-Ag-NPs, the amide band of pure chitosan (spectrum not given) was moved from 1643 and 1589 cm⁻¹ to 1635 and 1546 cm⁻¹, corresponding to the C=O stretching and N–H bending vibrations. An amino band at 1589 cm⁻¹ and a carbonyl band at 1631 cm⁻¹ were found in the CSB. When compared to CSB, the bands of CSB-Ag-NPs were moved from 1635 and 1546 cm⁻¹ to 1734 and 1589 cm⁻¹, respectively. This shows that key functional groups are involved in reducing silver nitrate to silver nanoparticles. Also, a narrower vibration band for the O–H group at 3265 cm⁻¹ of CSB-Ag-NPs compared to CSB and a shift in band position and intensity, confirming CSB-Ag-NPs formation.

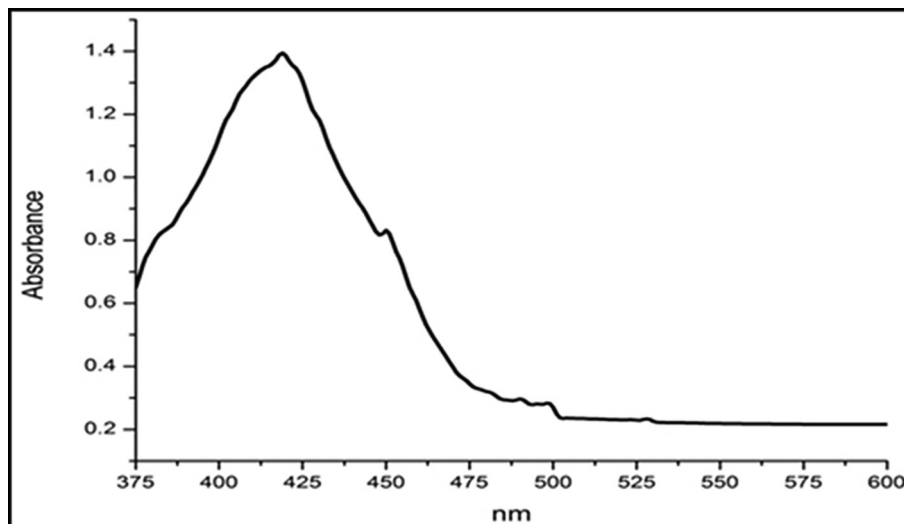


Fig. 1. UV-Vis spectra of CSB-Ag-NPs.

Table 1
FTIR details of chitosan Schiff base and CSB-Ag-NPs.

Wavenumber (cm ⁻¹)		Responsible groups
CSB	CSB-Ag-NPs	
3282	3265	N–H and O–H stretching vibration
2920	2873	
1635	1734	C = O stretching vibration
1546	1589	C=N and C=C stretching vibrations, N–H bending vibration
1381	1365	C–N stretching vibration
1151	1230	C–O–C skeletal linkage
1020	896	O–H, N–H bending vibration

3.3. XRD analysis

X-ray diffraction (XRD) was used for the analysis of molecular and crystal structures (Ali et al., 2022), qualitative identification (Ivanisevic, 2010), quantitative resolution (Cabral et al., 2013),

degree of crystallinity (Dey et al., 2009), isomorphous, substitutions (Ananias et al., 2013) and particle sizes (Singh et al., 2013). Fig. 3 represents the XRD pattern of chitosan and CSB-Ag-NPs. For pure chitosan, the XRD pattern shows two peaks at $2\theta = 9.9^\circ$ and 19.8° , which tells about the semicrystalline nature of chitosan (Fig. 3). The XRD pattern of CSB-Ag-NPs revealed the orientation and crystalline nature of silver nanoparticles (Fig. 3) along with the amorphous nature of CSB. According to the literature, the 2θ around 38° , 46° and 54° corresponded to the face-centered cubic Ag crystals' (111), (200) and (210) crystallographic planes (JCPDS file No. 04-0783), respectively (Palkumar et al., 2017). Similarly, for the PXRD profile of CSB-Ag-NPs, the 2θ values were seen at 38° , 46° and 54° , which corresponds to the presence of Ag-NPs with face-centered cubic structure, whereas the peak at $2\theta = 27^\circ$ related to CSB. Thus, the XRD analysis results confirmed the presence of silver nanoparticles in CSB with a face centered cubic lattice structure.

Comparing the XRD pattern of pure chitosan and CSB-Ag-NPs showed a broadness of peak and shift in peak position. This sup-

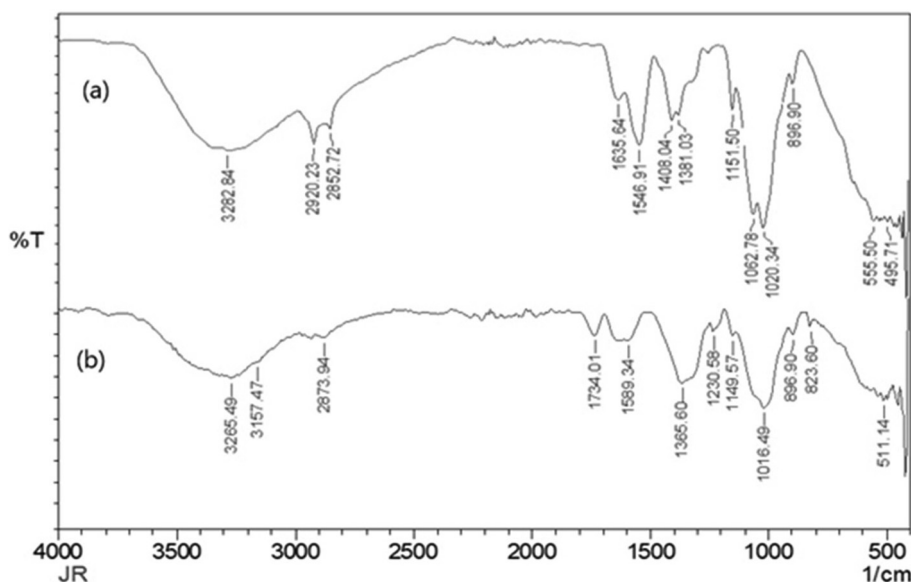


Fig. 2. FTIR spectrum of (a) CSB and (b) CSB-Ag-NPs.

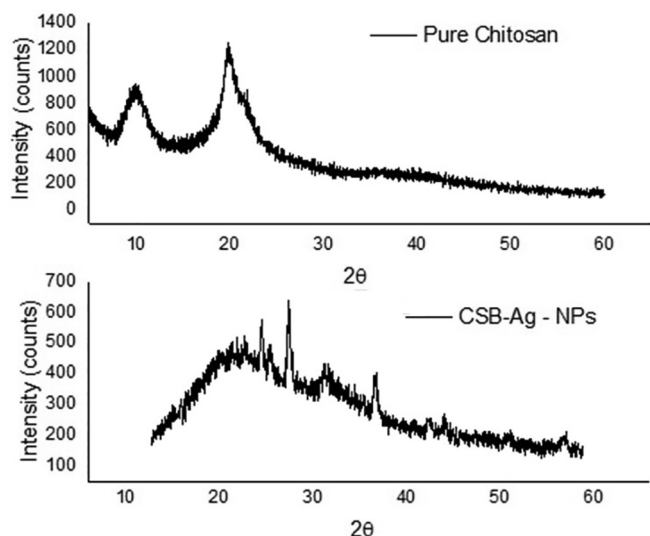


Fig. 3. XRD pattern of pure Chitosan and CSB-Ag-NPs.

ports the modification of pure chitosan. Also, the amorphous nature of CSB-Ag-NPs proves its suitability for various applications, especially in the biological field. The intense peak present in the amorphous environment reflects the presence of crystalline Ag nanoparticles. The broad peaks in the diffraction pattern indicate the small crystallite size (Wani et al., 2011). The size of the prepared silver nanoparticles was determined using Debye–Scherrer formula,

$$D = K \lambda / \beta \cos \theta$$

where 'D' is particle diameter size, k is a constant approximately equal to 1, λ is the wavelength of the X-ray source (1.54056 nm), ' β ' is the full width half maximum (FWHM) and θ is the diffraction angle corresponding to the lattice. The average particle size was estimated as a crystalline size of 3.8 nm, 9.02 nm, and 3.45 nm for different diffraction angles of silver nanoparticles. This demonstrates that CSB aids in the production of silver nanoparticles.

3.4. TEM analysis

Fig. 4 shows a TEM picture of CSB-Ag-NPs. The analysis confirmed the creation of Ag nanoparticles with spherical morphology and tiny aggregates, which ranged in size from 5 to 20 nm. The particle size determined by the Debye–Scherrer equation is supported by a TEM examination.

3.5. Porosity measurements

The porosity of the CSB-Ag-NPs was determined by the liquid displacement method. The measurement of porosity in terms of volume of void (0 to 1) and percentage (0 to 100) gives an idea regarding the characteristics of the materials. The porosity can be determined by measuring void spaces present in the materials (Glasbey et al., 1991). Voids are generally formed due to a phase transformation (Nakahara, 1977).

Scaffold porosity and pore size are important in biological and biomedical applications. Cell development and the flow transfer of nutrients and metabolic waste are both dependent on porosity (Elia et al., 2015). The cells would be able to travel in and populate the sample due to the high porosity. The porosity of the synthesized CSB-Ag-NPs was found to be nearly 53.24 %, by which it can be inferred that the sample has a medium porosity.

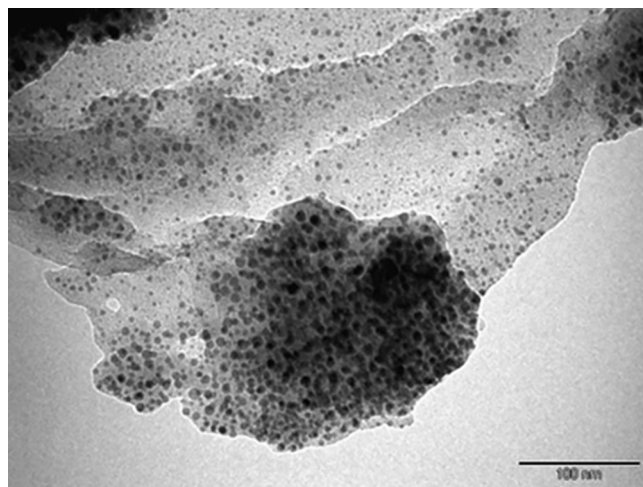


Fig. 4. TEM image of CSB-Ag-NPs.

3.6. Antioxidant assay

3.6.1. DPPH and H_2O_2 scavenging activity

Oxidation is the essential activity for all microorganisms to produce energy and fuel for biological processes. But some of the oxidants and free radicals are considered very toxic. They may cause damage to tissues and cells, so the antioxidant potential of synthesized CS and CSB-Ag-NPs was determined using DPPH and H_2O_2 scavenging methods. The DPPH is a stable free radical that is extensively used to estimate antioxidants' free radical-scavenging abilities. To determine antioxidant capability, the change in optical density of DPPH free radicals as compared to the change in concentration of CS and CSB-Ag-NPs. Due to the scavenging of DPPH by the donation of hydrogen to create the stable DPPH molecule, the methanolic solution of DPPH transformed blue to yellow when prepared material was added. The scavenging activity of the chitosan and CSB-Ag-NPs. In both methods was concentration-dependent (Fig. 5). Increase in concentration from 20 to 120 $\mu\text{g/mL}$, scavenging activity of chitosan (9.1 to 34.6% and 6.2 to 35.6%) and CSB-Ag-NPs (13.12 to 46.25% and 9.61 to 49.35%) were enhanced significantly in both DPPH and H_2O_2 method respectively. Chitosan and its derivatives, including CSB are well-known antioxidant materials (Guo et al., 2005). Also, silver nanoparticles have been evaluated as a potent antioxidant by researchers (Chokshi et al., 2016). The results obtained in this research work indicated that synthesized material CSB-Ag-NPs had great antioxidant potential against DPPH and H_2O_2 , which was obviously related to the presence of CSB and silver content in the nanoparticles than pure chitosan.

3.7. Antimicrobial activity

The disc diffusion method was used to determine the antibacterial and antifungal activity of chitosan and CSB-Ag-NPs, and activity was measured after 24 h by measuring the zone of inhibitions in millimeters. Chitosan and CSB-Ag-NPs have been tested for antibacterial activity against *E. coli*, *P. aeruginosa*, and *P. notatum*. Chitosan and CSB-Ag-NPs showed significant inhibitory activity against these strains of the microorganisms. The antimicrobial activities were compared against ampicillin (antibacterial) and polymyxin B sulfate (antifungal). The graphical representations of antibacterial and antifungal activities are shown in Fig. 6. Chitosan and its derivatives like CSB, trimethyl chitosan (TMC), etc., have already been studied as potent antimicrobial agents. Antibacterial and antifungal properties of silver nanoparticles are also widely

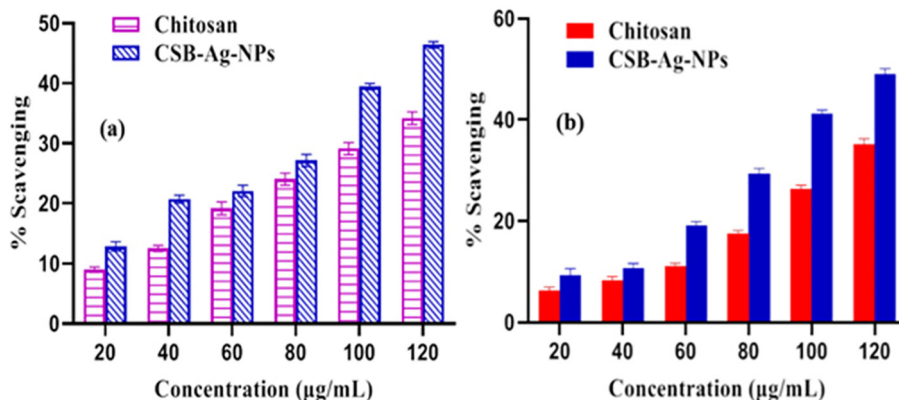


Fig. 5. Scavenging activity of chitosan and CSB-Ag-NPs (a) DPPH assay and (b) H₂O₂ assay.

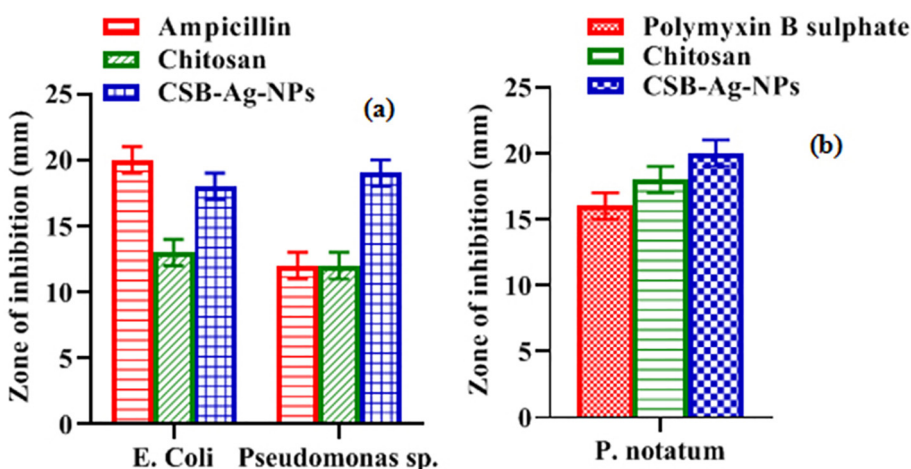


Fig. 6. Comparative antimicrobial activity of Chitosan and CSB-Ag-NPs (a) antibacterial activity and (b) antifungal activity.

applied in the medical, pharmaceutical, agricultural and biotechnological field. The enhanced antimicrobial activities of such compounds were observed due to increased permeability, hydrophilicity, solubility, lipophilicity and positively charged ions. This made easy penetration of molecules into the cell membrane and interrupted the cell respiration resulting in inhibition of protein synthesis and inhibition of microbial growth. Inhibition of bacteria's cell growth and lysis was observed due to the blockage of nutrient flow via the permeable cell of *B. cereus* (Visu Kumar et al., 2005). Recently reported that Schiff base stabilized Ag-NPs as a potential antibacterial agent (Minhaz et al., 2020). In this study, when chitosan was modified as CSB-Ag-NPs, its properties and applications could tend to be increased. Because of their small size, the modified CSB-Ag-NPs could easily access the microorganisms' nuclear content and have a vast surface area, allowing for extensive contact with them. The antibacterial and antifungal properties of silver nanoparticles were attributed to the interaction of Ag⁺ ions with bacterial DNA, causing cell growth and bacterial replication to be inhibited. The results obtained in this research work clearly indicated that synthesized material CSB-Ag-NPs had great antibacterial and antifungal potential, which was surely related to the presence of CSB and silver content in the nanoparticles.

3.8. Larvicidal bioassay

The larvicidal activity of CSB-Ag-NPs against *Culex Quinque fasciatus* fourth stage larvae was determined in this work, and mortal-

ity was recorded as a function of nanoparticle concentration. The larvicidal activity of CSB-Ag-NPs was shown to be concentration-dependent in our study. Nearly 40% mortality was reported at a dose of 3 mg/ml, which escalated to 90% at a dosage of 10 mg/ml (Fig. 7). AgNPs have already been explored as potent larvicidal by Elumalai et al. (2020), they found that novel biopolymer-inspired AgNPs were more efficient with respect to time and concentration. Also, Priyadarshini et al. (2012) demonstrated larvicidal and pupicidal activity of silver nanoparticles against *A. stephensi*, and reported the highest mortality in synthesized silver nanoparticles. Anand et al. (2014) found the larvicidal activity of chitosan NPs produced from crab and squilla species against *Aedes aegypti*. In the same way, Solairaj and Rameshthangam (2017) shown increased antibacterial and mosquito larvicidal activities using silver NPs incorporated in a -Chitin nanocomposite. Similar observations were found in the present study and concluded that the presence of chitosan and Schiff base has played a vital role in the enhancement of the larvicidal activity of silver NPs.

3.9. Safety of compounds (Toxicity assay)

Artemia salina, one of the most useful test organisms available for marine ecotoxicity testing, was used to conduct a biosafety assessment of CSB-Ag-NPs (Rajasree et al., 2011). For various concentrations such as 50, 100, and 200 g/mL, the half-maximum effective concentration (EC₅₀) test yielded a value of 166.16 (Glasbey et al., 1991). According to the previous findings, the tox-

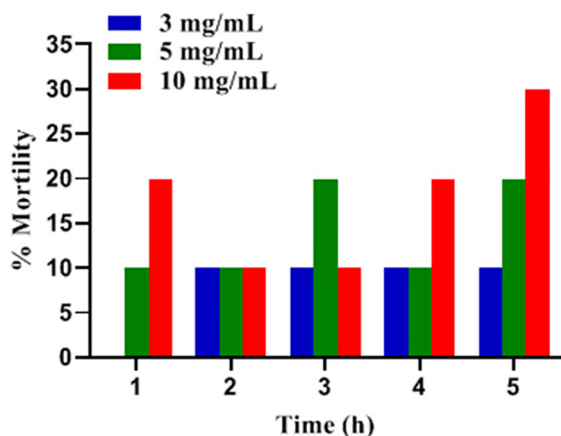


Fig. 7. Concentration-dependent larvicidal activity of CSB-Ag-NPs.

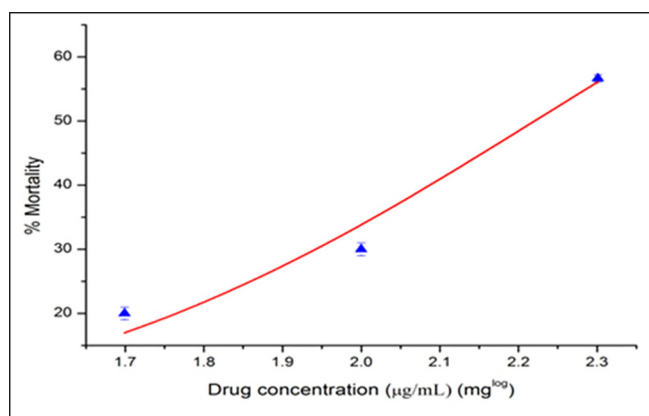


Fig. 8. Half maximal effective concentration test.

icity of silver nanoparticles to aquatic animals is dose-dependent (Asharani et al., 2008).

Like the primary data, the nanoparticle aggregates demonstrated considerable mortality within 24 h of exposure. When the concentration reached 200 g/mL, most *nauplii* (>50%) died. Therefore, it could be concluded that the death of the species was concentration-dependent. This might be because the gut of the species could have filled with NP aggregates that made less food available and resulted in death. Hence, this study reveals silver nanoparticles impregnated with chitosan Schiff base have an effect not only on the alive animal but also on cysts (Go et al., 1990). From the results (Fig. 8), it can be concluded that the mouthparts and the gut region appeared clear at minimum concentration, whereas at higher concentration, the entire gut region was accumulated with the sample and due to the high toxicity of the prepared CSB-Ag-NPs the tissue of the animal start degraded.

4. Conclusion

The CSB-Ag-NPs were successfully synthesized using chitosan Schiff base and the formation of nanoparticles was confirmed by UV-Vis and FTIR studies. The XRD pattern of the nanoparticles exhibited amorphous or crystalline nature, which helped increase the porosity of the material. The synthesized CSB-Ag-NPs showed good antioxidant, antibacterial, antifungal and larvicidal activity against selected species of the microbes. The safety bioassay revealed that the synthesized silver nanoparticles were non-toxic to the marine ecosystems at lower concentrations, but percentage

mortality was increased at higher concentrations. This report may inspire the utilization of chitosan Schiff bases and their CSB-Ag-NPs for biomedical and pharmaceutical applications.

Declaration of Competing Interest

The authors declare that they have no known competing financial interests or personal relationships that could have appeared to influence the work reported in this paper.

Acknowledgements

This work was financially supported by Taif University Researchers Supporting Project number (TURSP-2020/90), Taif University, Taif, Saudi Arabia.

References

- Abdul Rahuman, A., Gopalakrishnan, G., Venkatesan, P., Geetha, K., 2008. Isolation and identification of mosquito larvicidal compound from *Abutilon indicum* (Linn.) Sweet. *Parasitol. Res.* 102 (5), 981–988.
- Ali, A., Chiang, Y.W., Santos, R.M., 2022. X-ray Diffraction techniques for mineral characterization: a review for engineers of the fundamentals, applications, and research directions. *Minerals* 12 (2), 205.
- Anand, M., Maruthupandy, M., Kalaivani, R., Suresh, S., Kumaraguru, A.K., 2014. Larvicidal activity of chitosan nanoparticles synthesized from crab and squilla species *Against Aedes Aegypti*. *J. Colloid Sci. Biotechnol.* 3, 188–193.
- Ananias, D., Almeida Paz, F.A., Carlos, L.D., Rocha, J., 2013. Chiral microporous rare-earth silico-germanates: Synthesis, structure and photoluminescence properties. *Microporous Mesoporous Mater.* 166, 50–58.
- Asharani, P.V., Lian Wu, Y.i., Gong, Z., Valiyaveetil, S., 2008. Toxicity of silver nanoparticles in zebrafish models. *Nanotechnology* 19 (25).
- Badawy, M.E.I., Lotfy, T.M.R., Shawir, S.M.S., 2019. Preparation and antibacterial activity of chitosan-silver nanoparticles for application in preservation of minced meat. *Bull. Natl. Res. Cent.* 43, 83.
- Baran, T., Menteş, A., Arslan, H., 2015. Synthesis and characterization of water soluble O-carboxymethyl chitosan Schiff bases and Cu(II) complexes. *Int. J. Biol. Macromol.* 72, 94–103.
- Bin Ahmad, M., Lim, J.J., Shameli, K., Ibrahim, N.A., Tay, M.Y., 2011. Synthesis of silver nanoparticles in chitosan, gelatin and chitosan/gelatin bionanocomposites by a chemical reducing agent and their characterization. *Molecules* 16, 7237–7248.
- Cabral, M., Pedrosa, F., Margarido, F., Nogueira, C.A., 2013. End-of-life Zn–MnO₂ batteries: electrode materials characterization. *Environ. Technol.* 34, 1283–1295.
- Chokshi, K., Pancha, I., Ghosh, T., Paliwal, C., Maurya, R., Ghosh, A., Mishra, S., 2016. Green synthesis, characterization and antioxidant potential of silver nanoparticles biosynthesized from de-oiled biomass of thermotolerant oleaginous microalgae *Acutodesmus dimorphus*. *RSC Adv.* 6, 72269–72274.
- Dey, A., Mukhopadhyay, A.K., Gangadharan, S., Sinha, M.K., Basu, D., 2009. Characterization of microplasma sprayed hydroxyapatite coating. *J. Therm. Spray Technol.* 18, 578–592.
- Dutta, P.K., Dutta, J., Tripathi, V.S., 2004. Chitin and chitosan: Chemistry, properties and applications. *J. Sci. Ind. Res.* 63, 20–31.
- Elia, R., Michelson, C.D., Perera, A.L., Brunner, T.F., Harsono, M., Leisk, G.G., Kugel, G., Kaplan, D.L., 2015. Electrodeposited silk coatings for bone implants. *J. Biomed. Mater. Res. Part B Appl. Biomater.* 103, 1602–1609.
- Elumalai, K., Mahboob, S., Al-Ghanim, K.A., Al-Misned, F., Pandiyan, J., Baabu, P.M.K., Krishnappa, K., Govindarajan, M., 2020. Entomofaunal survey and larvicidal activity of greener silver nanoparticles: A perspective for novel eco-friendly mosquito control. *Saudi J. Biol Sci.* 27 (11), 2917–2928.
- Glasbey, C.A., Horgan, G.W., Darbyshire, J.F., 1991. Image analysis and three-dimensional modelling of pores in soil aggregates. *J. Soil Sci.* 42, 479–486.
- Go, E.C., Pandey, A.S., MacRae, T.H., 1990. Effect of inorganic mercury on the emergence and hatching of the brine shrimp *Artemia franciscana*. *Mar. Biol.* 107, 93–102.
- Guo, Z., Xing, R., Liu, S., Yu, H., Wang, P., Li, C., Li, P., 2005. The synthesis and antioxidant activity of the Schiff bases of chitosan and carboxymethyl chitosan. *Bioorganic Med. Chem. Lett.* 15 (20), 4600–4603.
- Hamidi, R., Jovanova, M., Kadifkova, B., Panovska, T., 2014. Toxicological evaluation of the plant products using Brine Shrimp (*Artemia salina* L.) model. *Maced. Pharm. Bull.* 60, 9–18.
- Hataf, N., Ghadir, P., Ranjbar, N., 2018. Investigation of soil stabilization using chitosan biopolymer. *J. Clean. Prod.* 170, 1493–1500.
- He, W., Liu, X., Kienzle, A., Müller, W.E.G., Feng, Q., 2016. In vitro uptake of silver nanoparticles and their toxicity in human mesenchymal stem cells derived from bone marrow. *J. Nanosci. Nanotechnol.* 16, 219–228.
- Ivanisevic, I., 2010. Physical stability studies of miscible amorphous solid dispersions. *J. Pharm. Sci.* 99, 4005–4012.

- Jin, X., Wang, J., Bai, J., 2009. Synthesis and antimicrobial activity of the Schiff base from chitosan and citral. *Carbohydr. Res.* 344, 825–829.
- Le Ouay, B., Stellacci, F., 2015. Antibacterial activity of silver nanoparticles: A surface science insight. *Nano Today* 10, 339–354.
- Lin, P.-C., Lin, S., Wang, P.C., Sridhar, R., 2014. Techniques for physicochemical characterization of nanomaterials. *Biotechnol. Adv.* 32, 711–726.
- Minhaz, A., Khan, N., Nargis Jamila, N., Javed, F., Imran, M., Shujah, S., Khan, S.N., Atlas, A., Shah, M.R., 2020. Schiff base stabilized silver nanoparticles as potential sensor for Hg(II) detection, and anticancer and antibacterial agent. *Arabian J. Chem.* 13, 8898–8908.
- Nakahara, S., 1977. Microporosity induced by nucleation and growth processes in crystalline and non-crystalline films. *Thin Solid Films* 45, 421–432.
- Oves, M., Rauf, M.A., Ansari, M.O., Warsi, M.K., Hussain, A., Ismail, I.I.M. 2021. 7 - Polysaccharide-based nanocomposites for gene delivery and tissue engineering, In: Bhawani, S.A., Karim, Z., Jawaid, M.B.T.-P.-B.N. for G.D. and T.E. (Eds.). Woodhead Publishing Series in Biomaterials. Woodhead Publishing, 103–129.
- Paulkumar, K., Gnanajobitha, G., Vanaja, M., Pavunraj, M., Annadurai, G., 2017. Green synthesis of silver nanoparticle and silver-based chitosan bionanocomposite using stem extract of *Saccharum officinarum* and assessment of its antibacterial activity. *Adv. Nat. Sci. Nanosci. Nanotechnol.* 8, 035019.
- Priyadarshini, K.A., Murugan, K., Panneerselvam, C., Ponarulselvam, S., Hwang, J.S., Nicoletti, M., 2012. Biolarvicidal and pupicidal potential of silver nanoparticles synthesized using *Euphorbia hirta* against *Anopheles stephensi* Liston (Diptera: Culicidae). *Parasitol. Res.* 111 (3), 997–1006.
- Rajasree, S.R.R., Kumar, G., Abraham, S., Dhinakaran, I., 2011. Studies on the toxicological effects of engineered nanoparticles in environment - A review. *Int. J. Appl. Bioeng.* 5, 35–45.
- Rezazadeh, N.H., Buazar, F., Matroodi, S., 2020. Synergistic effects of combinatorial chitosan and polyphenol biomolecules on enhanced antibacterial activity of biofunctionalized silver nanoparticles. *Sci. Rep.* 10, 1–13.
- Santhoshkumar, T., Rahuman, A.A., Rajakumar, G., Marimuthu, S., Bagavan, A., Jayaseelan, C., Zahir, A.A., Elango, G., Kamaraj, C., 2011. Synthesis of silver nanoparticles using *Nelumbo nucifera* leaf extract and its larvicidal activity against malaria and filariasis vectors. *Parasitol. Res.* 108 (3), 693–702.
- Silver, S., Phung, L.T., Silver, G., 2006. Silver as biocides in burn and wound dressings and bacterial resistance to silver compounds. *J. Ind. Microbiol. Biotechnol.* 33 (7), 627–634.
- Singh, D.K., Pandey, D.K., Yadav, R.R., Singh, D., 2013. A study of ZnO nanoparticles and ZnO-EG nanofluid. *J. Exp. Nanosci.* 8, 731–741.
- Solairaj, D., Rameshthangam, P., 2017. Silver nanoparticle embedded α -chitin nanocomposite for enhanced antimicrobial and mosquito larvicidal activity. *J. Polym. Environ.* 25, 435–452.
- Supriya Prasad, P., Gomathi, T., Sudha, P.N., 2017. Synthesis and characterization chitosan Schiff base (CSB) and its polyethylene glycol (PEG) blend. *Int. J. Nov. Trends Pharm. Sci.* 7, 57–63.
- Susilowati, E., Maryani, Ashadi. 2019. Green synthesis of silver-chitosan nanocomposite and their application as antibacterial material. *J. Phys. Conf. Ser.* 1153.
- Tong, J., Li, Z., Xia, C., 2005. Highly efficient catalysts of chitosan-Schiff base Co(II) and Pd(II) complexes for aerobic oxidation of cyclohexane in the absence of reductants and solvents. *J. Mol. Catal. A Chem.* 231, 197–203.
- Vishu Kumar, A.B., Varadaraj, M.C., Gowda, L.R., Tharanathan, R.N., 2005. Characterization of chito-oligosaccharides prepared by chitosanolytic with the aid of papain and Pronase, and their bactericidal action against *Bacillus cereus* and *Escherichia coli*. *Biochem. J.* 391, 167–175.
- Wang, R.M., He, N.P., Song, P.F., He, Y.F., Ding, L., Lei, Z.Q., 2009. Preparation of nano-chitosan Schiff-base copper complexes and their anticancer activity. *Polym. Adv. Technol.* 20, 959–964.
- Wang, W., Meng, Q., Li, Q., Liu, J., Zhou, M., Jin, Z., Zhao, K., 2020. Chitosan derivatives and their application in biomedicine. *Int. J. Mol. Sci.* 21 (2), 487.
- Wani, I.A., Ganguly, A., Ahmed, J., Ahmad, T., 2011. Silver nanoparticles: Ultrasonic wave assisted synthesis, optical characterization and surface area studies. *Mater. Lett.* 65, 520–522.
- Wei, D., Sun, W., Qian, W., Ye, Y., Ma, X., 2009. The synthesis of chitosan-based silver nanoparticles and their antibacterial activity. *Carbohydr. Res.* 344, 2375–2382.